Apoptosis Inducible Factor P53 Decrease Glutamate-Associated Damage via Inhibiting Ferroptosis

Zeyong Yang (yankylge@aliyun.com)
Shanghai Jiao Tong University School of Medicine
Wenting Xuan
Anhui Medical University
Yaru Jin
Anhui Medical University
Yuanhai Li
Anhui Medical University

Research

Keywords: p53, ferroptosis, neurodegenerative disease, glutamate-induced injury, neuron, neuroprotection

Posted Date: July 12th, 2021

DOI: https://doi.org/10.21203/rs.3.rs-680242/v1

Abstract

BACKGROUND: Ferroptosis, a pattern of programmed cell death decided by iron-associated lipid peroxidation, however, its role of p53-mediated xCT pathway in HT22 cell death remains obscure. Herein, this study is to investigate the potential mechanism of the effect of p53-mediated xCT pathway in HT22 cell lines in an iron-relevant mode.

METHODS: The viability of HT22 cells were detected by Cell Counting Kit-8(CCK-8) and PI/Hoechst fluorescence double staining. The protein expression levels of p53 and xCT were determined by western boltting. DHE fluorescence staining technique supervised the intracellular reactive oxygen species (ROS), and intracellular lipid oxidant situation was confirmed by BODIPY 581/591 C11 lipid peroxidation sensor. Intracellular ferrous ions were monitored with FeRhoNox™-1 fluoresceent probe.

RESULTS: The protein expression levels of p53 was obviously enhanced by tenovin-1 exposure. Accompanied with the upregulation of p53 protein, cell death was decreased significantly because of glutamate and erastin exposure with 8h, and p53-mediated xCT pathway was activated. Intracelluar ROS levels, lipid oxidant situations and ferrous ions were remarkably restricted from Glutamate-p53 groups in comparison with glutamate groups.

CONCLUSIONS: Overall, P53-mediated xCT pathway could decrease the glutamate-associated neurotoxicity, which may be relevant to the inhibition of ferroptosis.

Background

The term "ferroptosis" was first introduced in 2012 to describe an iron-dependent form of cell death caused by the accumulation of lipid-associated reactive oxygen species[(1)]. Iron metabolism represents a double-edged sword in most tissues, especially in the brain, which is extremely vulnerable to oxidation induced by excessive iron, resulting in possible destructive consequences. Just as recently indicated, stress can also lead to ferroptosis as well [(2)]. It is a new concept of death, which is different from the traditional mode of death. It is a cell regulatory necrosis characterized by iron and ROS dependence. In terms of cell morphology, biochemical indicators, and gene level, there are significant differences with other regulatory necrosis[(3)]. In recent years, iron death may play an important role in the development of many neurodegenerative diseases, such as Alzheimer's disease, Parkinson's syndrome and cerebral ischemic stroke. Iron death, an iron-dependent non-apoptotic cell death, could inhibit cystine/glutamate transporter, system xc(type I) or direct binding and inactivation through pharmacological action. Oxidation/iron death can lead to glutathione depletion and induce cell death.

Oxidative stress is associated with many neurodegenerative diseases. Oxidative stress caused by glutamate is an important inducement of neurodegenerative diseases. Glutamate damage model is a common model to study neuronal death induced by oxidative stress. High concentration of glutamate was used to incubate nerve cells to inhibit xCT, and thus inhibit the uptake of cystine, resulting in

intracellular glutathione (glutathione,GSH) deprivation and ROS accumulation[4]. Although Glutamate-induced neuronal death is mainly due to the accumulation of ROS in cells caused by GSH deprivation, it is not the only mechanism. Caspase-dependent apoptosis pathway is involved in the activation of 12-lipoxygenase (12-lipoxygenase, 12-lipoxygenase), translocation of apoptosis-inducing factor (apoptosis-inducing factor,AIF) and neurotoxicity induced by Glutamate[5]. In recent years, it was found that inhibition of iron death could inhibit glutamate-induced neuronal death in hippocampal slices[3].

P53 belongs to the p53 family, which mainly regulates cell cycle, induces apoptosis and DNA damage. p53 plays a key role in neurodegenerative diseases and aging[6]. Some studies have shown that p53 can increase the sensitivity of tumor cells to iron death by regulating the expression of xCT and thus play an anti-cancer role [7]. However, the effect of p53 on iron death in the nervous system is still unclear. Therefore, we used p53 specific activator Tenovin-1 in HT22 cell. The model of Glutamate damage was used to induce oxidative stress injury in some neurodegenerative diseases. We hypothesized that ferroptosis was decreased and glutamate-associated neurotoxicity was inhibited by P53-mediated xCT pathway in HT22 cells and its potential mechanism were investigated.

Materials And Methods

Cell and reagent

Cell and reagent HT22 cells (mouse hippocampal neuron cell line), donated by Professor Weilin Jin laboratory, Shanghai Jiaotong University. Fetal bovine serum, (from South America Lonsera company); DMEM/F-12 cell culture medium(American Hyclone company); 0.25% trypsin digestive juice(from Gibco company); Glutamic acid powder (No. 09581), Hoechst 33342 live cell dye (No. B2261), (from Sigma Inc., USA); Tenovin-1 (No. S8000, p53 specific activator); Erastin (No, S7242, Iron death-specific inducer, from Selleck Corporation), p53 antibody (No, 10442-1-AP, from Wuhan Sanying Corporation), 4-HNE (No, ab46545), xCT (No, ab175186, antibody, from Abcam Company, UK);β-actin, GAPDH antibody (from Santa Cruz Company, USA); FITC-labeled goat anti-rabbit antibody(from Beijing Zhongshanjinqiao Biotechnology Co., Ltd.); DHE fluorescent probe, cell proliferation test kit (cell counting kit-8,CCK-8, from Biyuntian Institute of Biotechnology); ECL light-emitting reagent kit; BODIPY™ 581/591C11 lipid oxidation probe (from Thermo Fisher, USA); FeRhoNox™-1 iron ion probe (from Goryochemical Corporation, Japan)

Instruments

Instrument fluorescence microscope (Leica Corporation, Germany); cell incubator (Thermo Corporation, America); enzyme labeling (Tecan Corporation, Germany); centrifuge (Beckman Corporation, Germany); protein electrophoresis, Bioshine ChemiQ chemiluminescence imaging system (Bio-Rad Corporation, America).

Experimental grouping

HT22 cells were randomly divided into 6 groups : (1) Control group(**CON**) : HT22 cells were cultured in DMEM/F12 medium; (2) p53 acitvation group (**P53**): HT22 cells were pretreated with 1 μ mol/L Tenovin-1 for 6 h, and HT22 cells were accompanied with p53 activation. (3) Glutamate exposure group (**Glu**): HT22 cells were treated with Glutamate with final concentration of 5 mmol/L; (4) Erastin treated group (**Era**): HT22 cells were treated with 0.5 μmol/L Erastin; (5) Glutamate exposure after p53 activation group(**p53-H**): After HT22 cells were adminitrated by 1 μmol/L Tenovin-1 for 6 h, and they were exposed to 5 mmol/L Glutamate. (6) Erastin-treated group (**Era-p53**): HT22 cells were pretreated with Tenovin-1 at the final concentration of 1 μmol/L for 6 h, and then they were administrated with 0.5 μmol/L Erastin.

RNA-seq Experiment

Total RNAs was quantified by the NanoDrop ND-2000 (Thermo Scientific) and the RNAs integrity was assessed using Agilent Bioanalyzer 2100 (Agilent Technologies).The sample labeling, microarray hybridization and washing were performed based on the manufacturer's standard protocols. Briefly, total RNAs were transcribed to double strand cDNAs and then synthesized cRNAs. Next, 2nd cycle cDNAs were synthesized from cRNAs. Followed fragmentation and biotin labeling, the 2nd cycle cDNAs were hybridized onto the microarray. After washing and staining, the arrays were scanned by the Affymetrix Scanner 3000 (Affymetrix).

Detection of HT22 cells viability

The viability of HT22 cells was detected by CCK-8 assay. HT22 cells were cultured in 96-well plates at about 1×10^4/ well for 12 h. Glutamate (final concentration was 1, 5, 10 mmol/Land Erastin (0.25, 0.5, 11 μmol/L were added. The control group and blank group (corresponding amount of cell culture medium and CCK-8 solution) were set up, each hole was set up 5 compound pores. After 6 hours of incubation in incubator, 10 μL CCK-8 solution was added to each well(100 μL medium per well). After incubated with 2 h in the incubator, the absorbance value of each well was measured at 450 nm wavelength by spectrophotometer, and the relative survival rate of each well was calculated. The relative survival rate = (experimental group - blank group) / (control group - blank group), the experiment repeated 3 times.

The protective effects of p53 activation on glutamate damage and iron death induced by erastin in HT22 cells.

The protective effects of p53 activation on glutamate damage and iron death induced by erastin in HT22 cells were detected by PI/Hoechst fluorescence double labeling method. HT22 cells were inoculated with 5×10^4 cells/well in 24-well plate and treated according to above-mentioned method. After treatment for 8 h, the final concentration of 5 mg/L Hoechst 33342 and PI solution were added to the medium. The cells were incubated with 37°C and 5% CO_2 for 10 min, and the relative cell survival rate was calculated under fluorescence microscope. Relative cell survival rate was expressed as the ratio of Hoechst /(Hoechst$^+$+PI$^+$) greater than 500 cells. The experiment was repeated three times.

Western blot was used to detect the difference of p53 and xCT protein expression.

Western blot was used to detect the difference of p53 and xCT protein expression. 1 ×10^5cells / well were vaccinated into 6-well plate for 12 h, then treated with different concentrations of Tenovin-1 (0.1, 1, 10μmol/L) for 6 h, and then the samples were prepared, and the samples were treated with different concentrations of p53 (0.1, 1, 10 μmol/L) for 6 h. The cells were washed twice by PBS and added with lysate containing protease inhibitors and phosphatase inhibitors. The cells were lysed on ice for 10 min, using a cell brush and scraped off the cells and placed in a 1.5 mL EP tube with ultrasound for 3 times for 5 s. BCA protein quantitative kit was used to detect the concentration of protein. The sample was mixed with 3×SDS buffer at 2:1 volume, boiled at 100℃for 5 min, quickly placed on ice to room temperature and centrifuged at 13000 × g for 5 min. After electrophoresis with 35 μg protein sample per well, the protein was transferred to the PVDF membrane at a constant current of 200 mA for 1 h, which was washed 3 times with 5% skimmed milk powder for 1 h. TBST was at room temperature, β-actin antibody was diluted at a dose of 1:1000 each time at room temperature for 1 h and 4℃overnight. After TBS washing 3 times, and 10 min each time. The cells were incubated at room temperature with 1:5 000 dilution for 1 h, developed with ECL kit and β-actin as internal reference; the expression level of xCT protein was detected: 1×10^5 cells per well were inoculated in 6-well plate for 12 h, and the cells were cultured for 12 h. After 8 hours of treatment, the samples were prepared according to the above method, and the expression level of xCT protein was detected by Western blot. XCT and GAPDH antibody were diluted by 1: 1 000.

The lipid oxidation product 4-HNE was detected by immunofluorescence assay.

The HT22 cells were seeded with 5×10^4 cells per well in 24-well plate. Control, P53, Glutamate and Glutamate-p53 group was selected for 8 h according to above-mentioned method. The cells were washed twice with PBS, fixed at room temperature with 4% paraformaldehyde for 15 min, washed 3 times with PBS, sealed with 15% donkey serum at room temperature for 1 h, washed with PBS for 3 times, and added with an antibody 4-HNE. The dilution ratio is 1:200, 4℃ overnight after incubation at room temperature for 1 h, washed for 3 times, added with second antibody (dilution ratio of 1:400), incubated at room temperature for 1 h, washed for 3 times, then sealed with 10 μg/ml DAPI glycerol, The average fluorescence intensity of different groups was observed under fluorescence microscope.

BODIPY 581/591 C11 lipid oxidation fluorescence probe was used to detect intracellular lipid oxidation

BODIPY 581/591 C11 lipid oxidation fluorescence probe was used to detect intracellular lipid oxidation in HT22 cells inoculated in 24-well plate with 5×10^4/well. Control, P53, Glutamate and Glutamate-p53 group

was selected for 8 h according to above-mentioned method. Methanol dissolved the BODIPY 581/591 C11 fluorescence probe to the storage solution with the concentration of 10 mmol/L, and added the final concentration of 1 μmol/L BODIPY 581/591 C11 fluorescence probe to the treated cells. The cells were incubated at 37℃ and incubated with a fluorescent probe of 1μmol/L BODIPY 581/591 C11. After incubating with PBS for 30 min, the unbound dyes were washed twice with PBS. The fluorescence effect was observed by fluorescence microscope, and the average fluorescence intensity of different groups was observed.

FeRhoNox-1 fluorescent probe was used to detect the changes of intracellular iron ions

FeRhoNox-1 fluorescent probe was used to detect the changes of intracellular iron ions in HT22 cells, which were vaccinated with 5×10^4 cells per well in 24-well plate. Control, P53, Glutamate and Glutamate-p53 group was selected for 8 hours according to the above-mentioned method. The FeRhoNox-1 fluorescent probe was dissolved into 1 mmol/L storage solution by DMSO. After being treated with 24-well plate, the cells were washed twice with PBS and diluted with HBSS solution to 5 μmol/L working solution. 200 μ L was added to each well. The working solution was incubated in 37℃, 5% CO_2 incubator for 1 hour, washed twice with HBSS solution and observed under fluorescence microscope. The average fluorescence intensity of each group was calculated.

Statistical analysis

The statistical analysis was carried out with SPSS 20.0.0 software. The measurement data were expressed as the mean ± SD from at least three biological replicates, and the comparisons between groups was performed by one-way ANOVA (Analysis of Variance), pairwise comparison using Tukey test. A value of $p < 0.05$ was considered statistically significant. Meanwhile, affymetrix GeneChip Command Console (version 4.0, Affymetrix) software was used to extract raw data. Next, Expression Console (version1.3.1, Affymetrix) software offered RMA normalization for both gene and exon level analysis. Then the gene expression analysis and alternative splice analysis proceeded separately. □ Gene expression analysis: Genesrping software (version 13.1; Agilent Technologies) was employed to finish the basic analysis. Differentially expressed genes were then identified through fold change as well as P value calculated with t-test. The threshold set for up- and down-regulated genes was a fold change > = 2.0 and a P value < = 0.05. Afterwards, GO analysis and KEGG analysis were applied to determine the roles of these differentially expressed mRNAs played in these GO terms or pathways. Finally, Hierarchical Clustering was performed to display the distinguishable genes' expression pattern among samples. □ Alternative splice analysis: Alternative splice analysis was conducted by Transcriptome Analysis Console (version1.0, Affymetrix). Differential exon or junction identified through splicing index as well as P value calculated with One-Way Between-Subject ANOVA (Unpaired). The threshold was splicing index > = 2.0 or < = -2.0

Results

RNA-seq indicated that p53 participated in glutamate-associated damage in HT22 cells

Principal component analysis (PCA): By means of PCA analysis, the distribution of the samples was investigated, the rationality of the experimental design was verified, and the homogeneity of the repeated biological samples was demonstrated by two-dimensional diagram(Figure 1A); Cluster analysis: Unsupervised hierarchical clustering of differentially expressed genes was performed(Figure1B); Pathway analysis: The differential genes were analyzed by pathway in KEGG database(Figur1C); Scattered point graph (matrix graph) was shown in Figure 1D.

Tenoin-1 could evoke an increase in the level of p53 protein in HT22 cells

Tenovin-1 induced the increase of p53 protein level in HT22 cells in a concentration-associated manner (included 0.1, 1 and 10 μ mol/L). P53 level in HT22 cells was enhanced at 6 h accompanied with Tenovin-1 exposure, and the p53 expression was increased at 6 h after Tenovin-1 treatment. Therefore, Tenovin-1 was pre-treated for 6 hours. The p53 protein level in HT22 cells treated with 1 μmol/L Tenovin-1 for 6 h was significantly higher than that in the control group($P < 0.05$). Therefore, 1 μmol/L Tenovin-1 was chose as the optimal concentration to induce p53 activation in subsequent experiments(Fig 2).

P53 inhibited the glutamate- and erastin-associated neurotoxicity of HT22 cells

P53 inhibited the glutamate and erastin-associated neurotoxicity of HT22 cells (1,5,10 mmol/L) in a concentration-dependent manner. When the concentration of glutamate was 5 mmol/L, the cell viability of HT22 cells was about 40%. Therefore, 5 mmol/L was chose as the appropriate damage concentration for subsequent experiments. After pretreatment with 1 μmol/L Tenovin-1 for 6 h, the cell death in HT22 cells could be obviously inhibited by glutamate stimulation ($P < 0.01$)(Fig 3A, 3C). In order to determine whether p53 can decrease iron death, the classical iron death inducer Erastin was used to induce iron death in HT22 cells, and the effect of p53 on the model was detected. Erastin (0.25, 0.5, and 1μmol/L) significantly inhibited the cell viability(Fig 3B, 3D). When erastin concentration was 0.5 μ mol/L, the survival rate of HT22 cells was about 35%. Therefore, 0.5 μmol/L was chosen as the suitable concentration for the subsequent toxic test. After exposure to 1 μmol/L Tenovin-1 for 6 h, the cell viability in HT22 cells were significantly rescued from erastin-induced cell death by p53 activation ($P < 0.01$).

P53 inhibited the increase of lipid oxidation in HT22 cells activated by glutamate.

After 8 h of glutamate exposure, the lipid oxidation level of HT22 cells was increased about 4 times compared with the control group, howerer, in Glu-p53 group, the level of lipid oxidation decreased significantly (P <0.01). After lipid oxidation, 4-HNE content (the product of cell lipid metabolism) of the cells was increased significantly(Fig 4A). Then glutamate was treated for 8 h, we found that the 4-HNE content was significantly higher than that of the control group (P <0.01). However,the level of 4-HNE in glutamate-p53 group was significantly lower than that in control group (P<0.01) (Fig 4B).

P53 inhibited the increase of intracellular iron ion in HT22 cells activated by glutamate

The concentration of divalent iron ion was increased by about 4 times in HT22 cells in glutamate group compared with the control group (P < 0.01), the intracellular iron concentration of HT22 in Glutamate-p53 group was significantly lower than that in control group (P <0.01) (Fig 5), which demonstrated that activation of p53 remarkably inhibited the increase of iron ion concentration induced by glutamate.

P53 reversed the inhibition of xCT expression induced by Glutamate and Erastin in HT22 cells

The expression level of xCT protein was decreased in glutamate group(P < 0.05) compared with the control group(Fig 6A). The expression of xCT protein in glutamate-p53 group was significantly higher than that in glutamate group (P < 0.05). In the classical iron death inducer Erastin damage model (Fig 6B), the expression of xCT protein was significantly inhibited in erastin group in comparison to the control group(P < 0.01), and which was also significantly increased in erastin-p53 group than that in erastin group (P < 0.01).

Dicussion

Iron death is a regulatory necrosis characterized by lipid oxidation and iron dependent pathway, which is different from traditional caspase-dependent apoptosis and cell necrosis. In recent years, studies have shown that iron death may be inextricably linked to Parkinson's disease, Alzheimer's disease, and Huntington's disease[8-10].

Some studies have shown that iron death is closely related to p53 activation in lung cancer and osteosarcoma, and this process mainly depends on the direct transcription inhibition of xCT (The main component of System Xc)[11]. Our results showed that p53 not only did not increase the sensitivity of glutamate-associated damage in HT22 cells, but also rescued cell viability from HT22 cell death. And we carried out further research to make sure the role of iron death.

Erastin, a classical iron death inducer, can induce iron death. We used tenvion-1 to pretreat with HT22 cells for 6 h to induce p53 activation, and then erastin was administrated to induce iron death. Our results

showed that the survival rate was significantly higher in erastin-p53 group than that of erastin group, which indicated that p53 pathway could restain from the iron death of HT22 cells. In order to verify whether p53 inhibits iron death in the glutamate-induced damage model and thus protect HT22 cells from glutamate-evoked neurotoxicity, we further explore the cell survival rate in T22 cells exosure to glutamate in the situation of both p53 activation and no p53 activation. It was found that the levels of ROS, lipid oxidation and divalent iron ion in glutamate-p53 group were significantly lower than those in glutamate group, which suggested that p53 could inhibit the iron death of HT22 cells and make HT22 cells exempt from the neurotoxicity of glutamate.

Since studies have shown that p53 increases the sensitivity of tumor cells to iron death in lung cancer and osteosarcoma cells may be due to the regulation of xCT protein expression[(6)]. In order to explore the possible mechanism of p53 resistance to iron death, we examined the expression of xCT protein in HT22 cells and found that the expression of xCT protein was inhibited in glutamate group and erastin group, which was also confirmed in the previous study[(12)]. In glutamate-p53 and erastin-p53 groups, the inhibition of xCT protein expression was reversed in a certain extent. It is suggested that xCT plays a key role in the inhibition of glutamate- and erastin-associated damage by p53 acitivation.

In our study, the role of p53 in neurodegenerative diseases and iron death was investigated mainly on HT22 cells. HT22 cell, a mouse hippocampal neuron line, which derived from HT4 cell lines, and adherent to the growth under normal conditions. Because of the lack of ion channel glutamate receptor, it is suitable to study the oxidative stress damage model of Glutamate, which is widely used in many degenerative diseases researches. However, there were some limitations, HT22 cell line is different from primary nerve cells and animal neurons, so the role of p53 in primary nerve cells and animals needs to be further excavated; Meanwhile, xCT is not silenced and the protective effect of p53-mediated xCT pathway is needed to further explored.

In conclusion, this study suggests that p53-mediated xCT pathway can protect neural celsl from the neurotoxicity of glutamate by inhibiting iron death, which provides a novel strategy to excavate the role and potential mechanism of p53 in many neurodegenerative diseases.

Abbreviations

CCK-8 Cell Counting Kit-8

ROS Reactive oxygen species

AIF Apoptosis-inducing factor

ANOVA Analysis of Variance

GO Gene Ontology

KEGG Kyotoencyclopedia of genes and genomes

PCA Principal component analysis

Declarations

Acknowledgments

This work was supported by the National Natural Science Foundation of China (No: 81401279); Shanghai Natural Science Foundation(No: 18ZR1443100), Shanghai Jiao Tong Unviersity School of Medicine, Innovation center of Translational Medicine Collaboration(No: TM201729); Youth Talent Fund of International Peace Maternity and Child Health Hospital, Shanghai Jiaotong University School of Medicine in 2014 (To Zeyong Yang) and Xinchen Foster Fund for Anesthesiologists in Shanghai (To Zeyong Yang).

Author Contributions

YZY and LYH designed the study. XWT, YZY, and JYR performed the experiments. YZY and LYH provided expertise and material. XWT, and YZY wrote the manuscript.

All authors read and approved the final version of the manuscript.

Data Availability

All data generated or analyzed during this study are included in this manuscript.

Conflict of interest

The authors declare that they have no conflict of interest.

Ethical Approval

This study included the use of HT22 cell line. No other biological samples derived from patients or laboratory animals were used. All procedures performed in studies involving human participants were in accordance with the ethical standards of the Shanghai Jiao Tong University research committee and with the 1964 Helsinki Declaration and its later amendments or ethical standards.

References

1. Hirschhorn T, Stockwell BR. The development of the concept of ferroptosis. Free Radic Biol Med 2019; 133:130-143.
2. DeGregorio-Rocasolano N, Martí-Sistac O, Gasull T. Deciphering the Iron side of Stroke: Neurodegeneration at the Crossroads Between Iron Dyshomeostasis, Excitotoxicity, and Ferroptosis. Front Neurosci. 2019; 19:13:85.

3. Dixon SJ, Lemberg KM, Lamprecht MR, Skouta R, Zaitsev EM, Gleason CE, Patel DN, Bauer AJ, Cantley AM, Yang WS, Morrison B 3rd, Stockwell BR. Ferroptosis: an iron-dependent form of nonapoptotic cell death. Cell, 2012;149: 1060-1072.
4. Kang Y, Tiziani S, Park G, Kaul M, Paternostro G Cellular protection using Flt3 and PI3Kα inhibitors demonstrates multiple mechanisms of oxidative glutamate toxicity. Nat Commun, 2014; 5:10.1038
5. Xu X, Chua CC, KongJ, Kostrzewa RM, Kumaraguru U, Hamdy RC, Chua BH. Necrostatin-1 protects against glutamate-induced glutathione depletion and caspase-independent cell death in HT-22 cells. J Neurochem, 2007; 103:2004-2014.
6. Checler F, Costa C A. p53 in neurodegenerative diseases and brain cancers. Pharmacol Ther, 2014; 142: 99-113.
7. Jiang L, Kon N, Li T, Wang SJ, Su T, Hibshoosh H, Baer R, Gu W Ferroptosis as a p53-mediated activity during tumour suppression. Nature, 2015; 520: 57-62.
8. Hambright WS, Fonseca RS, Chen L, Na R, Ran Q. Ablation of ferroptosis regulator glutathione peroxidase 4 in forebrain neurons promotes cognitive impairment and neurodegeneration. Redox Biol, 2017; 12: 8-17.
9. Chen L, Hambright WS, Na R, Ran Q Ablation of the Ferroptosis Inhibitor Glutathione Peroxidase 4 in Neurons Results in Rapid Motor Neuron Degeneration and Paralysis. J Biol Chem,2015; 290: 28097-28106.
10. Van D B, Gouel F, Jonneaux A, Timmerman K, Gelé P, Pétrault M, et al., Ferroptosis, a newly characterized form of cell death in Parkinson's disease that is regulated by PKC. Neurobiol Dis, 2016; 94: 169-178.
11. Wang SJ, Li D, Ou Y, Jiang L, Chen Y, Zhao Y, Gu W. Acetylation Is Crucial for p53-Mediated Ferroptosis and Tumor Suppression. Cell Rep, 2016; 17: 366-373.
12. Stockwell BR, Friedmann Angeli JP, Bayir H, Bush AI, Conrad M, Dixon SJ, et al., Ferroptosis: A Regulated Cell Death Nexus Linking Metabolism. Redox Biology, and Disease. Cell, 2017; 171: 273-285.

Figures

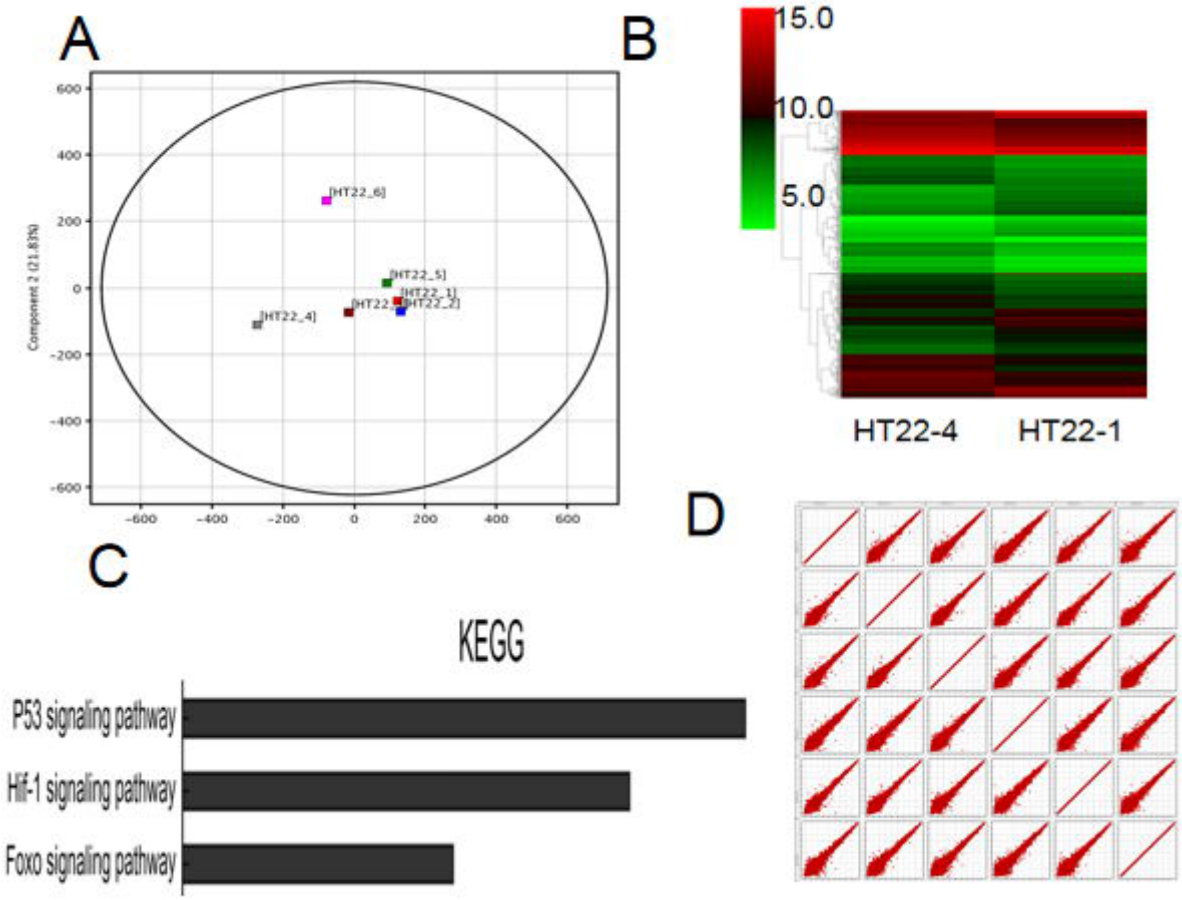

Figure 1

RNA-seq information in HT22 cells The samples of the same group were concentrated in the two-dimensional spatial distribution, indicating that the selection of these genes was representative and the biological duplication was good(Figure 1A); The distance between the two pairs of samples is calculated to form a distance matrix. The two nearest classes of distance are combined into a new class, and the distance between the new class and the current class is calculated, then merged and calculated until there is only one class. The expression of selected differentially expressed genes was used to calculate the direct correlation of the samples. In general, the same samples can be clustered in the same cluster, and the genes clustered in the same cluster may have similar biological functions. Display with Heatmap(Figure1B). The significance of gene enrichment in each pathway entry was calculated by statistical test. The calculated results return a significantly enriched P value, and a small p value indicates that the differential gene is enriched in the pathway. We can find out that p53 pathway may be related to the differentially expressed genes in different samples(Figur1C). The scatter plot of chip data is often used to evaluate the trend of two sets of data distribution centralization (Figure 1D).

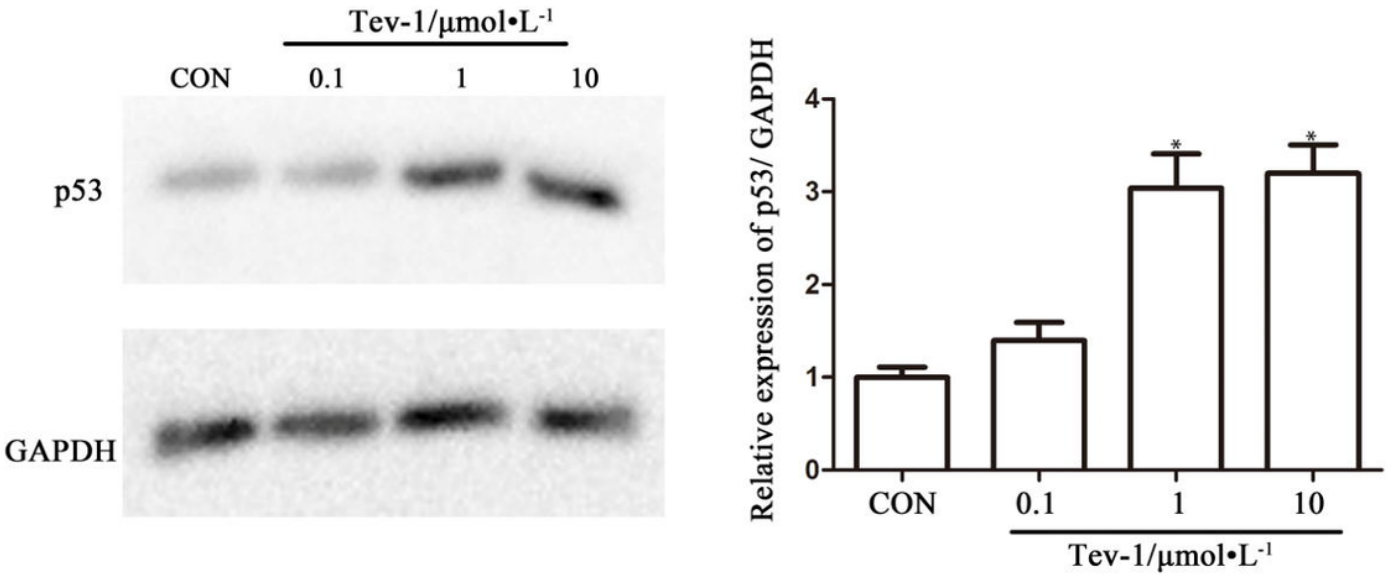

Figure 2

Tenovin-1 induced protein levels of p53. P53 were detected and quantified relative to GAPDH by western blot analysis. And relative amount of expression of p53 protein was statistically analyzed in HT22 cells(included 0.1, 1 and 10 μ mol/L). The p53 protein level in HT22 cells treated with 1 μmol/L Tenovin-1 for 6 h was significantly higher than that in the control group(Figure 2). Error bars: standard error of mean. Data were obtained from at least three separate cultures, given as mean ± SEM, and analyzed by two-way ANOVA followed by Bonferroni multiple comparison tests . *P<0.05 vs control.

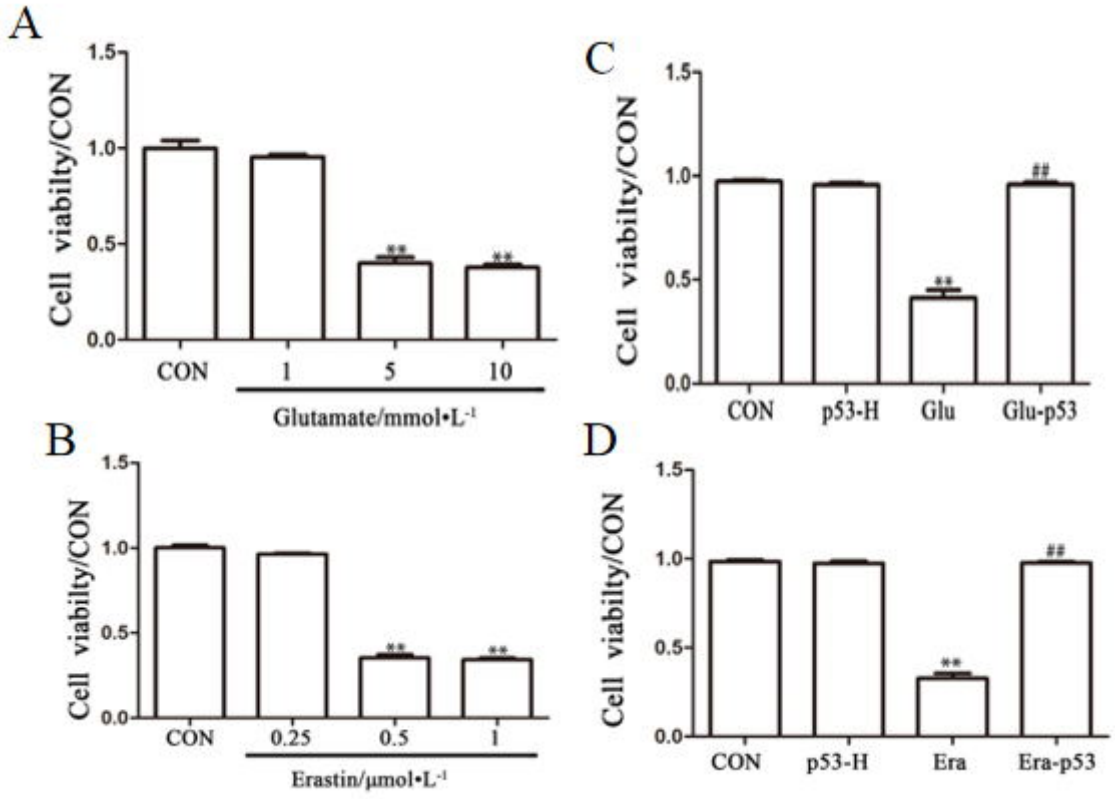

Figure 3

HT22 cells' viability were inhibited by different concentration Glutamate and erastin, p53 attenuated damage induced by glutamate and Erastin in HT22 cells Glutamate reduced survival rate of HT22 cells(Fig 3A) and p53 attenuated damage induced by glutamate in HT22 cells(Fig 3C); Erastin decreased survival rate of HT22 cells(Fig 3B) and p53 attenuated damage induced by Erastin in HT22 cells(Fig 3D). Error bars: standard error of mean. Data were obtained from at least three separate cultures, given as mean ± SEM, and analyzed by two-way ANOVA followed by Bonferroni multiple comparison tests . **P<0.01 vs control; ##P<0.01 vs glutamate, respectively.

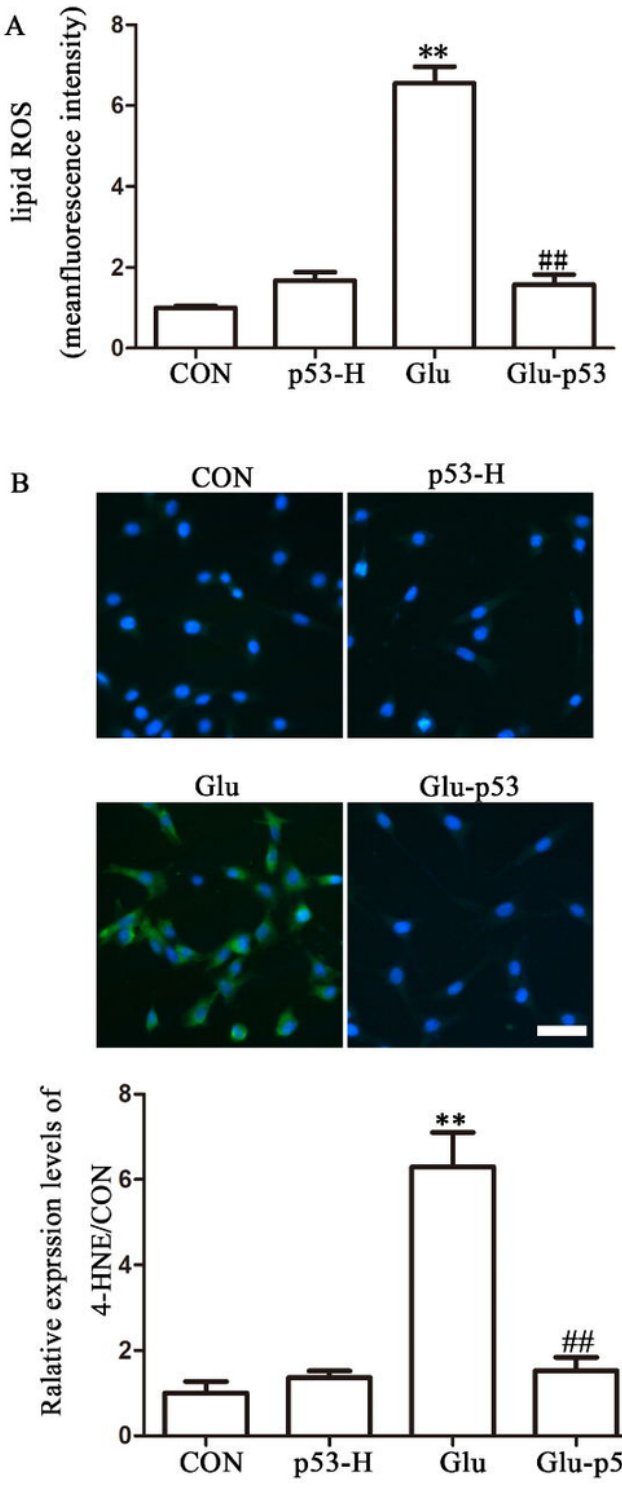

Figure 4

p53 decreased intracellular lipid oxidation evoked by glutamate. Fluorescence intensity of lipid oxidation in HT22 cells was decreased by p53 compared with glutamate group (##P<0.01 vs Glu.)(Figure 4A). Meanwhile, glutamate could increase the intracellular lipid oxidation. The average fluorescence intensity of each group was calculated; The lipid oxidation product 4-HNE was detected by immunofluorescence assay in HT22 cells (Figure 4B). p53 decreased expression of 4-HNE in HT22 cells induced by glutamate (Figure 4B) (scale bar=100 μm). Error bars: standard error of mean. Data were obtained from at least three separate cultures, given as mean ± SEM, and analyzed by two-way ANOVA followed by Bonferroni multiple comparison tests . **P<0.01 vs control; ##P<0.01 vs glutamate, respectively.

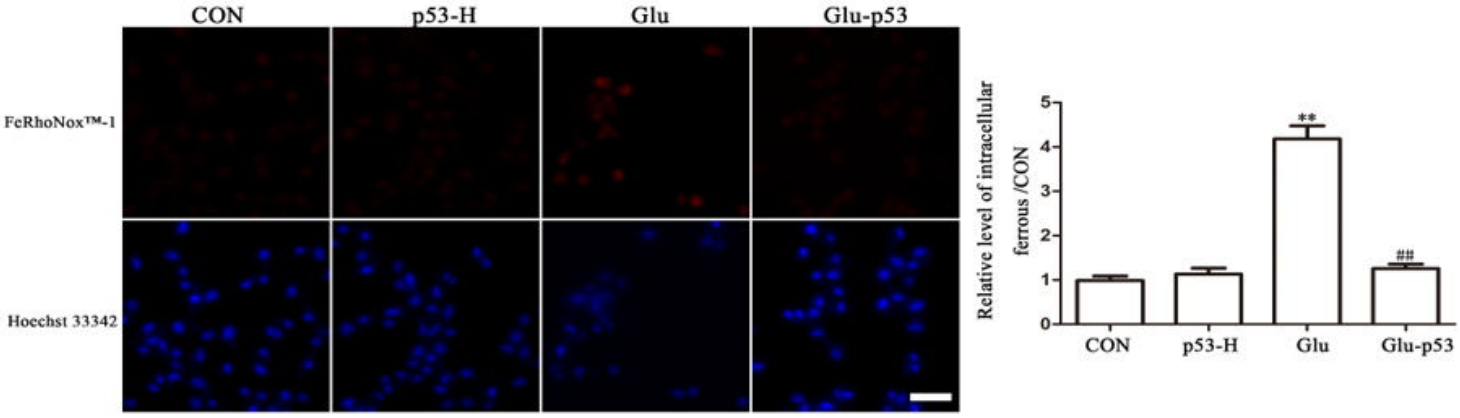

Figure 5

p53 reduced intracelluar ferrous level in HT22 cells activated by glutamate. FeRhoNox-1 fluorescent probe was used to detect the changes of intracellular iron ions in HT22 cells in control group, p53-H group, glutamate group and glutamate-p53 group. The average fluorescence intensity of each group was calculated, which indicated that p53 reduced intracelluar ferrous level in HT22 cells activated by glutamate(Figure 5). Error bars: standard error of mean. Data were obtained from at least three separate cultures, given as mean ± SEM, and analyzed by two-way ANOVA followed by Bonferroni multiple comparison tests . **P<0.01 vs control; ##P<0.01 vs Glu, respectively.

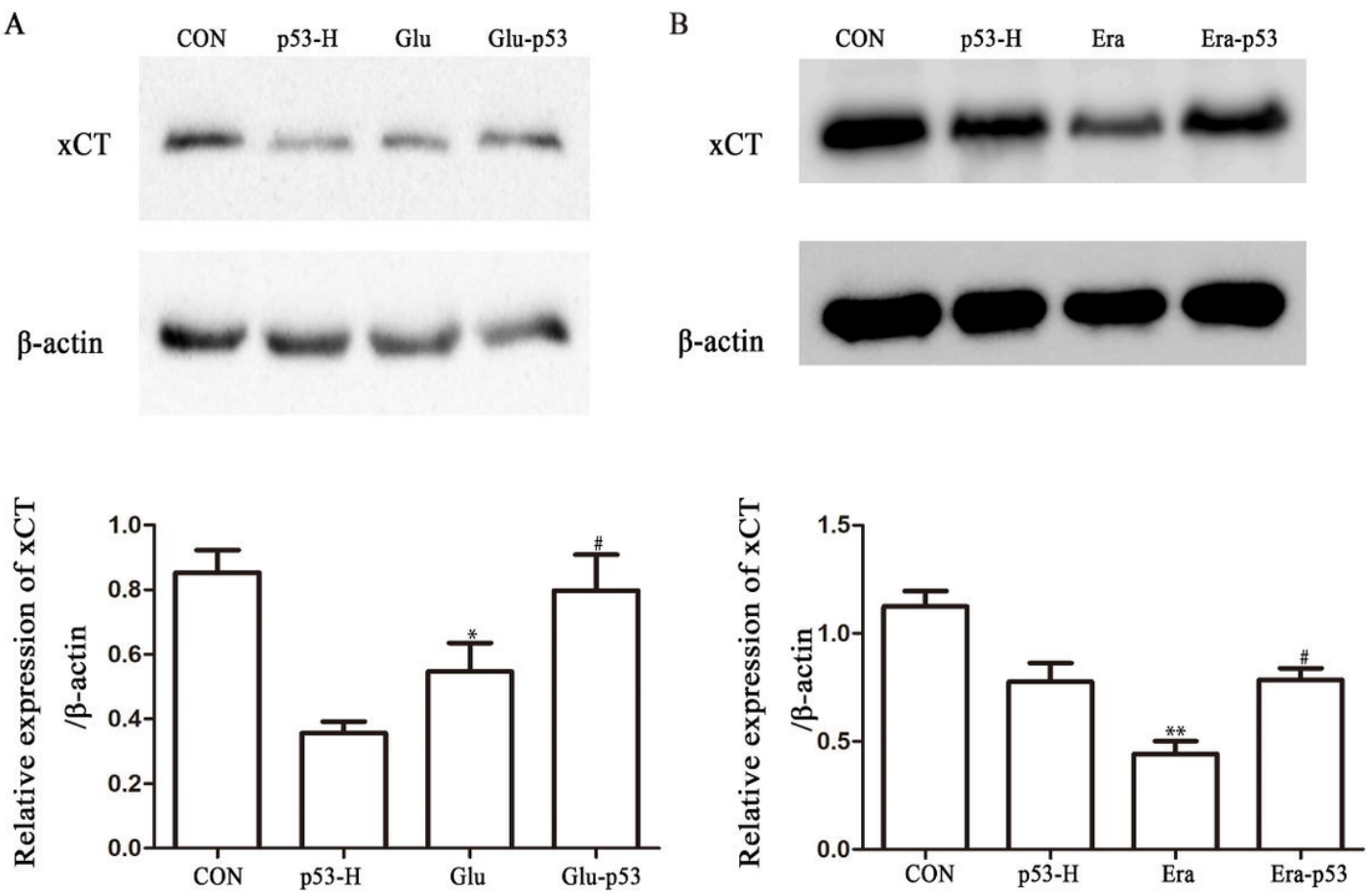

Figure 6

p53 reversed from suppression of the expression of xCT protein in HT22 cells acitivated by glutamate and erastin. p53 were detected and quantified relative to β-actin by western blot analysis. And relative amount of expression of xCT protein was statistically analyzed in HT22 cells in control group, p53-H group, glutamate group and glutamate-p53 group, which indicated that p53 increased expression of xCT in HT22 cells reduced by glutamate. Error bars: standard error of mean(Fig 6A). p53 were detected and quantified relative to β-actin by western blot analysis. And relative amount of expression of xCT protein was statistically analyzed in HT22 cells in control group, p53-H group, era group and era-p53 group, which indicated that p53 increased expression of xCT in HT22 cells reduced by erastin(Fig 6B). Error bars: standard error of mean. Data were obtained from at least three separate cultures, given as mean ± SEM, and analyzed by two-way ANOVA followed by Bonferroni multiple comparison tests . #P<0.05 vs Glu; **P<0.01vs CON, respectively.